

A Non-intrusive Multi-parameter Fault Diagnosis System for Industrial Machineries

Shanqing Wang¹, Chengpei Tang², Chancheng Zhou³, Xiaolong Zheng^{4*}

¹School of Engineering, Sun Yat-sen University, Guangzhou, China

²School of Engineering, Sun Yat-sen University, Guangzhou, China

³School of Data and Computer Science, Sun Yat-sen University, Guangzhou, China

⁴School of Computer Science, Beijing University of Posts and Telecommunications, Beijing, China

wangshq9@mail2.sysu.edu.cn, tchengp@mail.sysu.edu.cn, zhouchch6@mail2.sysu.edu.cn, xiaolong@greenorbs.com

Abstract—Induction motor, especially driving motor, is the critical component for various modern industrial machineries. Fault diagnosis of induction motor is therefore a necessary and crucial task to ensure the machinery health and prevent vital damages. Conventional diagnosis methods are mainly based on intrusive sensors to measure certain physical parameters. However, intrusive sensors are costly and hard to apply to update traditional machines. In this paper, we propose EMFD, an energy-image based non-intrusive multi-parameter fault diagnosis system. We design an EMFD sensing platform to monitor the electric circuit parameters. Then we build a fault model that describes the relationships between two major kinds of faults and the electric circuit parameters. Based on the model, we propose a novel fault diagnosis algorithm that exploits a sparse auto-encoder based deep neural network. Different from the existing single-parameter methods, EMFD takes advantage of multiple circuit parameters and achieves accurate and robust diagnosis even in dynamic operating environments. We implement and deploy the proposed system in a real-world factory. The evaluation results show that EMFD can achieve the diagnosis accuracy of 96%.

Index Terms—Fault diagnosis, electric power data, energy-image system, deep neural network, edge computing.

1

I. INTRODUCTION

Induction motors, as the core actuating devices, play an essential role in modern industry. Especially in large-scale pipelining production factory, driving motor used in industrial machinery is crucial for production automation, as shown in Fig. 1. Hence, the mechanical health and normal operation of driving motors are necessary and crucial. The eccentricity and breakage of rotor bar are two major common concerned faults for driving motors. The rotating rotor keeps producing centrifugal force and can run into harmful eccentricity when the rotating center axis continues deviating from the initial position [1]. Besides, the rotor bars with a limited service life can break due to overload and poor maintenance. Once those faults occur, the whole production line will malfunction and even damage, resulting in huge amount of financial loss and even casualties. According to statistic data, in China, about 200,000 motors break down every year and it costs more than 2 billion RMB to repair the motors. Fault diagnosis of the motors, to find the faults in time before more serious damage, is therefore indispensable for machineries in model industry.

¹* Corresponding author is Xiaolong Zheng.

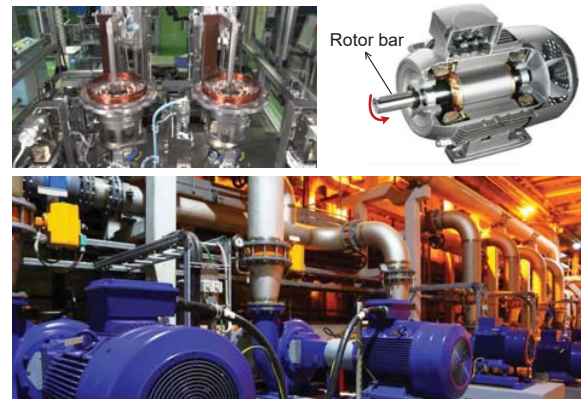


Fig. 1. Driving motors are widely used in a lot of industrial machineries.

Conventional fault diagnosis techniques are mainly based on intrusive sensor to analyze the vibration [2], [3], rotational speed [4], axial radial flux [5], etc. However, the embedded sensors have unaffordable costs in many cases. Lots of traditional machines have no data acquisition instrument to provide the newly raised diagnostic data. Upgrading those machines is a very serious challenge because usually no space inside the machine is reserved to add the intrusive sensors. Besides, the intrusive sensor can also be damaged and off-line when faults occur. Interruption of diagnostic data will cause failures to report the vital faults in time.

The proliferation of Internet of Things (IoT) brings novel solutions for traditional industry [6]. Recently, researchers find that the current variation, which can be acquired outside the machine, can reflect the operating condition of the machine [7]. However, the current can also fluctuate due to the instability of power supply and sudden changes of the load. Using a single parameter as the diagnosis evidence is not robust, leading to false alarms that interrupt the production and cause financial loss. In addition, most of existing methods manually select the classification features based on experience. The data can be underutilized when inappropriate features are used. The universality of the trained classification model is also limited, especially for different machines operating in dynamic operating environments.

In this paper, we propose EMFD, an Energy-image based non-intrusive Multi-parameter Fault Diagnosis system for industrial machineries. We take advantage of Internet of Things (IoT) and artificial intelligence techniques to solve above-mentioned problems. To enhance the data richness, we design an EMFD sensing device to collect various circuit parameters, including three-phase current, three-phase voltage, power and power factor. We call the set of circuit parameters collected during the same time period as an energy image. The energy image can show the operation condition, similar to a photo presents the human appearance. We further build a new model to describe the relationship between the operation condition and consecutive energy images, just like learning the human movements based on the video formed by serial photos.

Based on the fault diagnosis model, the edge servers of EMFD system perform a deep-learning based fault diagnosis algorithm to estimate the machine operating condition. We propose a sparse auto-encoder based deep neural network that automatically extracts diagnosis features, avoiding the limitations of manual feature selection in exiting classification-based diagnosis methods. To deal with dynamic operating environments, EMFD can integrate an online model adjustment method. While performing diagnosis, the edge serves forward the energy images to the cloud server for model training and updating. Then the cloud server will transmit the new model parameters to the edge serves. By this way, the edge servers can use limited computation resources on fault diagnosis to provide results in time. And the cloud server exploits the advantages of its abundant computation resources to train and update the model.

The contributions of this work are summarized as follows.

- We design a practical non-intrusive multi-parameter fault diagnosis system that uses IoT techniques to solve fault diagnosis problem in traditional industry. We implement a hardware platform to collect electric circuit parameters and build the novel diagnosis model that detects vital faults of rotors by those parameters.
- We propose a deep learning based fault diagnosis algorithm that exploits a sparse auto-encoder based deep neural network to automatically extract the circuit features, avoiding inappropriate features manually selected by existing classification-based methods.
- We implement and deploy our proposed system in a factory of Zhongjian Steel Structure Co., Ltd., in Huizhou, China. Based on the data collected from the real-world system, the evaluation results demonstrate the effectiveness of our system. The results show that the overall fault detection accuracy is 96%.

The rest of this paper is organized as follows. We will present the related works in Section II and elaborate our design details in Section III. We evaluate the system performance in Section IV and finally conclude our work in Section V.

II. RELATED WORK

To improve the reliability, stability and the economical efficiency of motor systems, early breakdown maintenance

has gradually turned into conditioned-based maintenance and predictive maintenance [8] that detect the faults in time and prevent the vital damages. Fault diagnosis of motor is a challenging task due to the complexity of induction motors and cross-correlation between faults. Existing methods usually rely on intrusive measurements. The authors in [9] design the ARM-based diagnosis systems and leverage the wavelet packet algorithm to analyze the operation condition. Data fusion technique is exploited in [10] to integrate multiple sensor readings for motor fault diagnosis. All of the sensor-based methods face two problems: difficulty to upgrade the deployed traditional machines, and data interruption caused by the sensor damages.

Existing non-intrusive diagnosis methods usually adopt classification algorithms to distinguish the normal and fault states. To extract features for classification, signal processing methods are adopted [11]. In paper [12], the authors exploit short-time Fourier transform to obtain the continuous frequency spectrum of quasi-stationary vibration signal as the feature. In [13], [14], empirical mode decomposition is used to process the sensor data for feature extraction. Wavelet transform and wavelet packet transform are also used to extract fault feature quantity [15], [16]. Nevertheless, selection of features relies on domain-specific knowledge and experience. It is hard to establish a well-trained model for various kinds of motors operating in dynamic environments. Different from the existing methods, we focus on exploiting the new deep learning techniques to automatically extract the appropriate features.

Motor Current Signature Analysis (MCSA) proposed in [17]–[19] uses the current signal as the key parameter to detect motor faults. Results in [20] have revealed the relationship between the current spectrum characteristics and the motor faults. Since current can be obtained more easily without affecting the normal operation of the motor system [18], MCSA is becoming popular. However, solely using current is not robust because the instability of power supply and power load can also cause current fluctuations.

III. SYSTEM DESIGN

In this section, we elaborate our design of EMFD, the energy-image based non-intrusive multi-parameter fault diagnosis system for industrial machineries. We first present the system overview (Section III-A) and then the self-designed EMFD device (Section III-B). We establish a fault diagnosis model (Section III-C) that describes the relationship between faults and the energy-image data. Based on the model, we propose a fault diagnosis algorithm (Section III-D) based on the sparse auto-encoder based deep neural network.

A. Overview

In a factory, machines are deployed in several workshops. The power supply in industry is usually three-phase power with a voltage of 390V. In each workshop, a electric brake is used to independently controls the power supply of the workshop. For each machine, a switch is also equipped to control the power on-off.

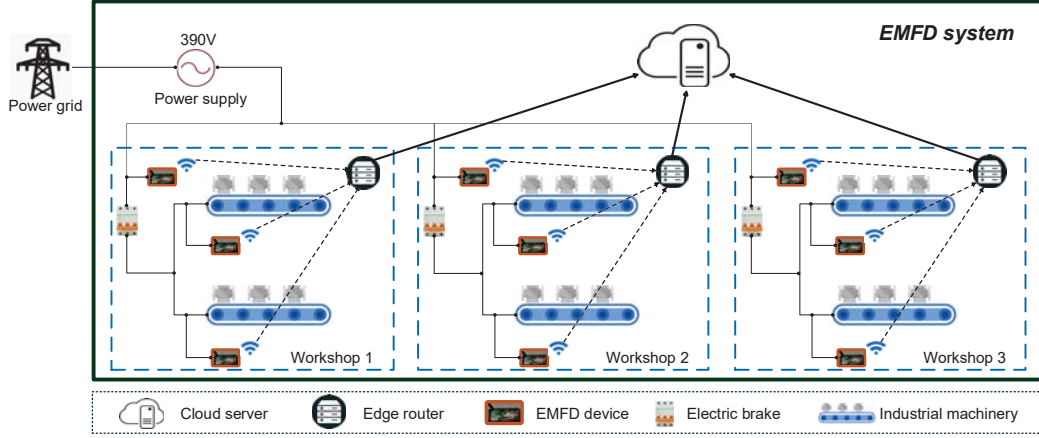


Fig. 2. Framework of EMFD.

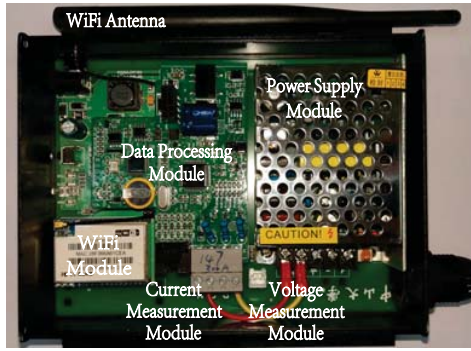


Fig. 3. The EMFD sensing device.

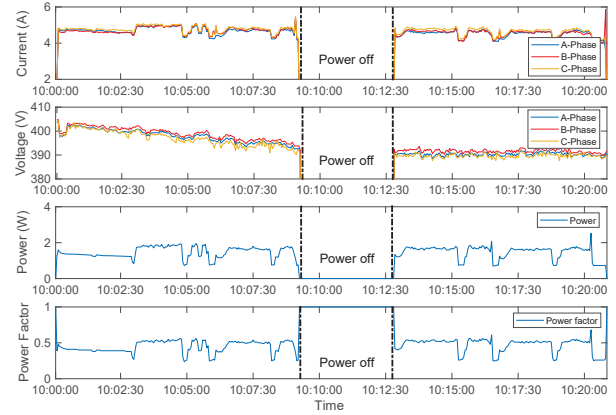


Fig. 4. Electric data collected by the EMFD device in our deployed system.

The framework of EMFD is shown in Fig. 2. The EMFD system consists of the EMFD sensing devices, edge routers and the cloud server. An EMFD sensing device integrates several sensors to collect the current and voltage of the power circuit and calculates the corresponding power and power factor, to form an energy-image frame. The device sends energy images to the edge routers via WiFi module. The edge routers perform in-suit fault diagnosis based on a sparse auto-encoder based deep neural network.

The edge routers forward the energy-image data to the could server for model updating. In EMFD, the diagnosis model is trained and updated at the could server to fully take advantage of the abundant computation resources. If any model parameter needs update, the could server transmit the updated parameters to the corresponding edge server. Note that the edge servers may run different models for different machines, to enhance the robustness in various operating environments.

B. Energy-image Sensing Device

To obtain more rich diagnosis data, we design an energy-image sensing device (EMFD device) to collect the electric circuit parameters, including three-phase current, three-phase

voltage, power consumption, and power factor. The power is defined as the sum of three-phase loads and the power factor refers to the the ratio of active power to apparent power. Fig. 3 shows the internal structure of our EMFD device. Besides the sensing modules, the sensing device also has data processing module for simple data preprocessing, WiFi module for data transmissions, and the power supply module.

The size of an EMFD device is $15.2cm \times 11.6cm \times 4.4cm$, which is small enough to be easily deployed in the workshops. The current, voltage, power, and power factor collected during the same period form an energy image. The sampling rate can be configured according to different requirements. In the default setting of our deployed system, the sampling rate is one energy image every three seconds. The EMFD device can check the data integrity and automatically sample again if the collected data is of poor quality. Hence, the data that an device reports to the router can be regarded as reliable.

We deploy our EMFD system in a factory of Zhongjian Steel Structure Co., Ltd., in Huizhou, China and collet the electric

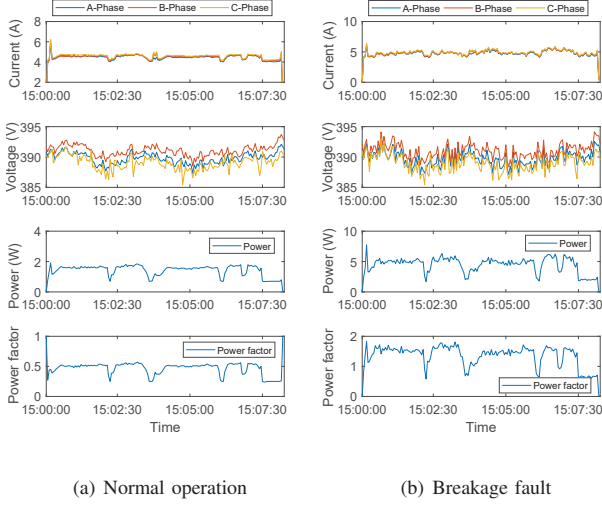


Fig. 5. Electric data during normal operation and rotor bar breakage fault.

circuit data from the real-world operation of a radial drill. Our EMFD system provides the 24/7 fault diagnosis service. We continuously collect the data for three days and obtain a data set of 86,400 energy images. During the three days, the radial drill operates in a good condition. Hence, the collected data are normal operation data. Fig. 4 shows a fragment of the collected data as an example.

C. Relationship between Faults and Circuit Parameters

In this section, we investigate the fault model that describes the relationship between the rotor bar breakage/eccentricity faults and the electric circuit data. How to use multiple parameters to robustly reflect the machine operation condition is crucial to our system design. Intuitively, electrical characteristics including current fluctuations and the increase of voltage harmonics can reveal general induction faults. But the exact fault model still need investigation.

Fig. 5 shows the electric data during normal operation and rotor bar breakage fault. According to previous study [21], when rotor bar breakage happens, two characteristic frequency components of the three-phase power called left-right variable frequency components will appear on the both sides of fundamental frequency component, at the frequency of $(1 + 2s)f_s$ and $(1 - 2s)f_s$, where s is slip ratio and f_s is the fundamental frequency of three-phase power supply. In China, the fundamental frequency of three-phase power supply is 50Hz and therefore the left and right variable frequency components of the radial drill are 25Hz and 70Hz. The amplitude of the left-right variable frequency components will vary with the breakage severity. The more serious the breakage of the rotor bar, the larger the amplitudes of the components.

When there is an eccentricity fault in the motor, there will also be two characteristic frequency components in the stator winding. Fig. 6 shows the electric data during normal operation and eccentricity fault. Different from the fault frequency for rotor bar breakage fault, the frequencies of eccentricity

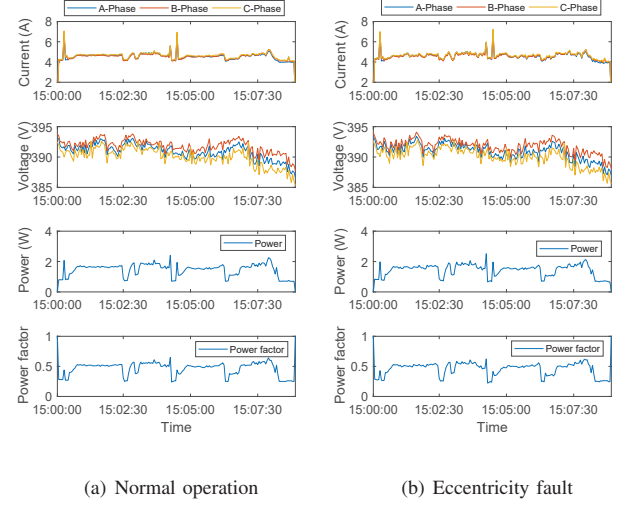


Fig. 6. Electric data during normal operation and eccentricity fault.

fault are $f_1 - f_r$ and $f_1 + f_r$, where f_1 is fundamental frequency and f_r is the rotating frequency of rotor. If we further take the torque and the fluctuation of revolving speed generated by the interaction between the aforementioned current and air-gap field into consideration, we can deduce fault frequencies are actually $f_1 \pm m f_r$, where m is a positive integer [22]. In our deployed system, the components with biggest amplitude during eccentric faults occurs at the frequency of $f_1 - f_r = 25Hz$ and $f_1 + f_r = 64Hz$.

In this section, we only present the characteristic relationships between faults and circuit parameters to demonstrate the feasibility of using multiple circuit parameters. To fully utilize the data, EMFD depends on the diagnosis algorithm to automatically extract the appropriate features.

D. Multi-parameter Fault Diagnosis Algorithm

Most of existing fault diagnosis methods are based on classification techniques that define a set of features in advance and train a classifier to detect the faults. Those methods require domain-specific knowledge to assess and select the appropriate features. But during the motor operation, the operating environment can be dynamic and expert-involved fault diagnosis is inefficient to adjust. What's worse, like in our application scenarios, new sensing data are included but cannot be fully utilized until a pansophic expert provides new determined domain-specific model depicting the relationships between faults and the newly included sensing data.

Thanks to the explosive development of artificial intelligence, machine learning techniques enable mining the inner features of data from mass data autonomously, eliminating the dependency on the experts. The relationships between faults and electric parameters revealed in prior section also shed the light on leveraging machine learning techniques to extract effective inner features to identify faults.

In this work, we proposed a deep-learning based fault diagnosis algorithm that exploits the sparse auto-encoder based

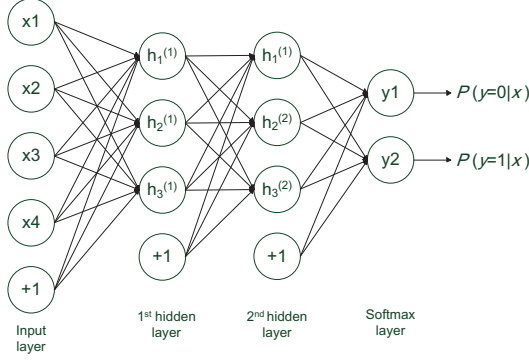


Fig. 7. Structure of SAE based DNN.

deep neural network (SAE based DNN). Sparse auto-encoder (SAE) is a neural network that is able to automatically learn sparse features from data by minimizing reconstruction error of input data and output data. During the training with only normal operation data, we want the output value of SAE approximately equals to the input value. When a fault occurs, circuit data go through the trained SAE will get an output value that is quite different from the input value. By this way, EMFD can detect the faults with only normal operation data.

We denote the m -th energy image data as $EI_m = \{I_m, V_m, p_m, pf_m\}$, where I_m , V_m , p_m , and pf_m are the m -th sample of current, voltage, power value, and power factor value, respectively. We feed the data set EI to the SAE based DNN for automatic feature learning. In the hidden layers, features are expressed as $F(EI_m, W, b)$. W is the set of weights between two neighboring layers and b refers to the bias in SAE.

We first use the unlabeled raw energy image data to train the required unsupervised features of the first hidden layer of SAE. Fig. 7 presents the structure of the proposed SAE based DNN. Each circle of hidden layers represents a hidden node. The automatical feature learning process is as follows:

- Step 1. Set the initial parameters of the neural network. Here we set the initial sparsity penalty term as 3, the initial decay parameter as 10^{-4} and the initial desired average activation of the hidden units as 0.3. The weights and bias of connections between the hidden nodes, W and b , are randomly selected and close to 0.
- Step 2. We adopt the batch gradient descent method as the forward propagation algorithm, to train the neural network. We compute the sparse cost function of each iteration of the layer according to the following equation.

$$J_{sparse}(W, b) = \frac{1}{N} \sum_{i=1}^N \left(\frac{1}{2} \|F_{w,b}(\rho(i))\|^2 \right) + \lambda + \beta \sum_{j=1}^{N_2} KL(\rho || \rho_j) \quad (1)$$

where $KL(\rho || \rho_j) = \rho \log \frac{\rho}{\rho_j} + (1-\rho) \log \frac{1-\rho}{1-\rho_j}$ is the kernel difference of two vectors, and $\rho_j = \frac{1}{n} \sum_{i=1}^n (a_j(\rho(i)))$ refers to the average activation of hidden unit j . λ is the weight decay parameters and N_2 is the number of the network nodes of the hidden unit.

- Step 3. We use Eq. (2) to update the weight W and Eq. (3) to update the bias b at each iteration of gradient descent updating.

$$W_{ij}(l) = W_{ij}(l) - \alpha \frac{\partial}{\partial W_{ij}(l)} cost(W, b) \quad (2)$$

$$b_i(l) = b_i(l) - \alpha \frac{\partial}{\partial b_i(l)} cost(W, b) \quad (3)$$

where α refers to the learning rate of the neural network, and l refers to the number of hidden layer.

- Step 4. To train network node in the second hidden layer, we repeated Step 2 and Step 3. The training process will finish when the maximum iteration round is reached or the value of cost function reached its minimum. The default maximum iteration round is set to 400. After training the SAE deep neural network, we use this built network model for online fault diagnosis.

The features learned by SAE in our EMFD system include the parameters in time domain, frequency domain, and non-linear domain. The time-domain parameters consist of mean value, standard deviation, and coefficient of variation. The frequency-domain parameters include low frequency power, high frequency power, low frequency power, high frequency power ratio, and total power. The nonlinear-domain parameters include approximate entropy, sample entropy, fuzzy entropy. The obtained parameters are applied for the reconstruction of the fault diagnosis model by the SAE automatically.

We use the cloud to train the model and update the system parameters. The uploaded data are processed to update the deep neural network parameters, neuron nodes. The operating environments of machines are not constant in the practical industrial factories. Besides, with the increase of the service time and the aging of the machine, the pre-trained classification model may become no longer suitable to obtain the satisfied diagnosis accuracy. Hence, we use online adjustment to match the natural state of the machine in real time by adjusting the network parameters and weights. Then the updated parameters are transmitted back to the edge servers to perform in-situ fault diagnosis.

IV. EVALUATION

In this section, we evaluate the EMFD system based on the real-world system deployed in a factory of Zhongjian Steel Structure Co., Ltd., in Huizhou, China. We will introduce the evaluation methodology and show the performance of EMFD, compared with existing methods that use a single parameter.

A. Methodology

To assess the performance of EMFD system, we consider three metrics: accuracy, sensitivity, and specificity. The definitions are shown in following equations, respectively.

TABLE I
PERFORMANCE OF EMFD WITH DIFFERENT NUMBER OF HIDDEN NODES IN TWO LAYERS.

Hidden nodes of layer 1		10	10	20	20	20	50	50	50	50	100	100	100	100	100
Hidden nodes of layer 2		5	10	5	10	20	5	10	20	50	5	10	20	50	100
Results	Accuracy(%)	83.91	85.02	88.06	89.22	88.24	90.74	91.09	93.68	95.84	91.36	92.13	93.22	96.31	94.99
	Sensitivity (%)	86.19	86.78	88.72	89.54	87.82	91.07	91.36	93.17	94.91	91.51	91.93	92.67	96.24	95.03
	Specificity (%)	81.63	83.26	87.39	88.90	88.66	90.41	90.83	94.17	96.76	91.21	92.34	93.76	96.39	94.95

TABLE II
PERFORMANCE OF THE SINGLE-PARAMETER BASED METHOD WITH DIFFERENT NUMBER OF HIDDEN NODES IN TWO LAYERS.

Hidden nodes of layer 1		10	10	20	20	20	50	50	50	50	100	100	100	100	100
Hidden nodes of layer 2		5	10	5	10	20	5	10	20	50	5	10	20	50	100
Results	Accuracy(%)	74.46	76.19	76.19	77.57	80.93	80.74	86.28	90.64	89.70	87.96	92.43	85.54	86.29	87.91
	Sensitivity (%)	74.01	74.64	76.94	76.40	80.44	79.71	86.64	89.61	90.55	87.40	91.89	89.79	85.39	87.04
	Specificity (%)	75.51	77.74	75.45	78.74	81.41	81.76	85.92	91.66	88.85	88.51	92.97	81.30	87.21	88.78

$$Accuracy = \frac{N_{tp} + N_{tn}}{N_{tp} + N_{tn} + N_{fp} + N_{fn}} \quad (4)$$

$$Sensitivity = \frac{N_{tp}}{N_{tp} + N_{fn}} \quad (5)$$

$$Specificity = \frac{N_{tn}}{N_{tn} + N_{fp}} \quad (6)$$

where N_{tp} , N_{tn} , N_{fp} , and N_{fn} refer to the classification numbers of true positive, true negative, false positive, and false negative, respectively.

We use the real-time electric data set collected by the mentioned EMFD devices for experiments. To validate the trained model, we construct the training set and test set. The collected real-world data are randomly divided into the training set and test set, with a ratio of 9:1. During our real-world deployment, we collect the data for three days and obtain a continuous electric power data with a size of 86400. Before sending to the edge routers, the EMFD sensing nodes will first preprocess the raw data with the following steps. First, using min-max normalization algorithm to normalize the raw data set to the range from 0 to 1. Second, dividing the electric series into multiple segments. Each segment has a length of 10 seconds.

After preprocessing, 8640 segments with the same length are obtained. Note that during our data collection period, the deployed system has no fault and only normal operation data are available. Even though our methods do not rely on labeled fault data to train the diagnosis model, we should have fault data to test our method. Hence, we generate the fault data based on domain-specific models. The generated fault data are verified by domain-specific experts from the factory and therefore credible to test the performance of EMFD system.

B. Performance Comparison with Single-Parameter Methods

Deep learning algorithms achieve different performances with different number of network layers and the number of hidden nodes in each layer. Generally speaking, the more layers and the more nodes in each layer, the better performance can be achieved. But the efficiency will degrade because of the exponential increase of the required computation resources. Hence, to ensure the diagnosis accuracy as well as the efficiency of EMFD, appropriate numbers of layers and nodes need to be set. In our EMFD system, we set the number of hidden layers to 2. Here, we vary the number of nodes in two layers to investigate the performance of EMFD.

Table I shows the results of EMFD. From the results, we can find that when the number of one layer is fixed and we increase the number of nodes in another layer, the accuracy doesn't necessarily increase all the time. Hence, we can select the setting that achieves the best performance as the default setting of EMFD system. When using 100 nodes in layer 1 and 50 nodes in layer 2, the diagnosis accuracy is 96.31%.

To demonstrate the robustness of our multi-parameter diagnosis model, we compare the performance of the method that uses a single parameter, current. Since SAE can achieve better performance than traditional classification algorithms, we improve existing single-parameter methods by integrating our SAE learning algorithm to automatically select the features of current. The data used is single-phase current extracted from our real-world data set. The size of the data set is also 8640 segments. A neural network model based on current is established and trained with the real-world data. The fault diagnosis performance is shown in Table II.

From the results in Table II, we can find the accuracy also first increases and then decreases with the number of

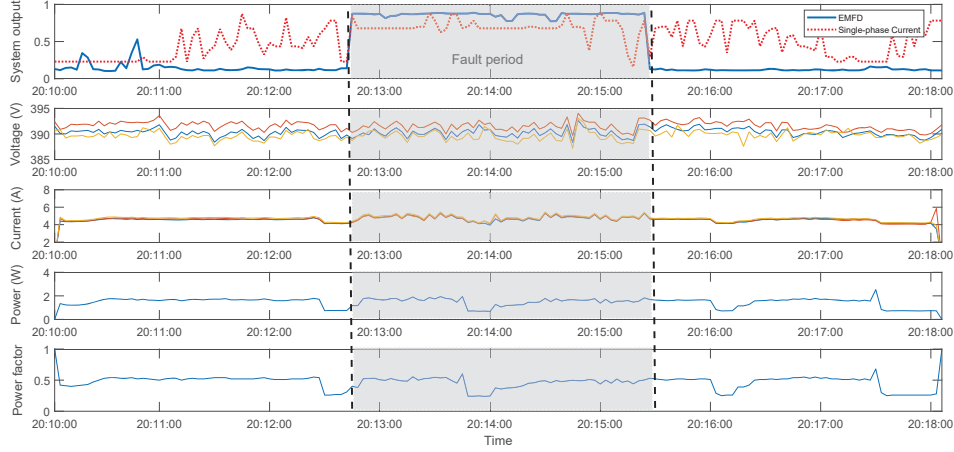


Fig. 8. Fault diagnosis results of EMFD and the single-parameter based method in our deployed system.

nodes increases. But the best performance are obtained with a different setting. When using 100 nodes in layer 1 and 10 nodes in layer 2, the accuracy is the best among all the results, which is 92.43%.

By comparing the single-parameter results in Table II and the multi-parameter results in Table I, we can find that the multi-parameter method has a better fault diagnosis accuracy. This is because more information is used to improve the robustness and accuracy. Note that the performance of existing methods with traditional classification algorithms is even worse than the tested single-parameter method in our paper because we improve it. The results demonstrate EMFD can effectively improve the performance of existing methods that use a single parameter.

In our current deployed system, we set the numbers of hidden nodes in the first and second layers as 100 and 50, respectively. The experiment results reveal a balance between accuracy and calculation speed. If a higher accuracy is desired, we can increase the numbers of hidden nodes and even the number of hidden layers. But the computational hardware should be upgraded if the diagnosis speed is also desired. In a nutshell, the proposed system is general for different application systems and we only present our deployed system, as an illustration. The model in our system can be adjusted based on user preferences when extending to other systems.

C. Robustness

Using multiple parameters can also enhance the robustness of diagnosis. We present the real-time system outputs of EMFD and the single-parameter method, together with the sensing data in Fig. 8. The system output is the probability of fault occurrence. The system decides a fault occurs when the probability exceeds a threshold. The threshold is also decided by the learning algorithm automatically.

In Fig. 8, the machine operates normally in from 20:10:00 to 20:12:45 and then encounters faults since 20:12:45. The faults continue until 20:15:30 and the machine recovery to normal

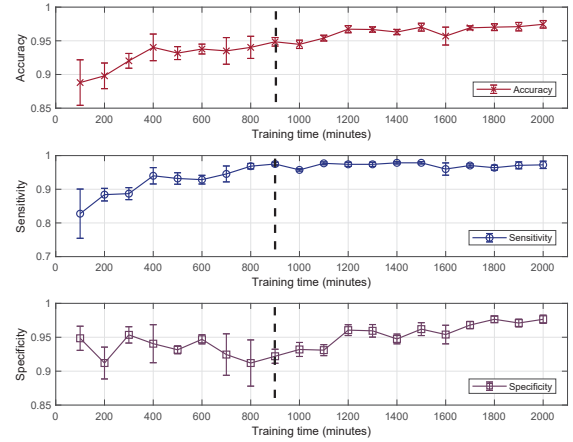


Fig. 9. Performance under different training time.

condition since then. We can find the system output of EMFD keeps low during normal operations and sharply increases to a very high probability when the fault occurs. The results show that EMFD can accurately distinguish the normal operations and faults. However, we can see that the system output of the single-parameter method has large variations even during the normal operations. The probabilities of fault occurrences during fault period and normal operation period are very similar when using only current as the diagnosis evidence. Hence, using a single parameter is inaccurate, consistent to the results in Table I and Table II. From the results, we can draw the conclusion that EMFD is more robust than existing single-parameter methods.

D. Convergence Time

Convergence time is important for learning-based methods. EMFD adopts online model updating and needs fully training the model only when the machine runs for the first time. Once the model is trained, only light-weight updating but

not the time-consuming full training is needed. Therefore, the convergence time is calculated as the training time to get a stable model with limited performance variations. We evaluate the performance of EMFD with different training times. For each training time, we repeat the experiments 10 times and calculate the average, worst and best performance. The evaluation results are shown in Fig. 9. From the results, we can find the performance is improved with the increase of training time, as expected. And after a certain training time (900 minutes), the performance becomes stable with limited variations. Compared with the machine lifetime, which is usually several years, the 15-hour training cost is totally acceptable.

V. CONCLUSION

In this paper, we propose EMFD, an energy-image based non-intrusive multi-parameter fault diagnosis system for industrial machineries. Instead of using the operating data collected by intrusive sensors embedded in the machines, we use the electric parameters of the power supply lines to detect the motor faults. We build the fault model to depict the relationships between two major kinds of rotor faults and the electric circuit parameters. Based on the model, we design a novel deep-learning based fault diagnosis algorithm. We exploit a sparse auto-encoder based deep neural network to automatically extract the features, avoiding the dependency on domain-specific knowledge in existing methods. We leverage the edge computing to perform timely fault diagnosis in situ and leave the model training and updating tasks to the cloud that has abundant computation resources. By this way, EMFD is robust even in the dynamic operating environments. We implement and deploy a real-world system based on our proposed methods, in a factory of Zhongjian Steel Structure Co., Ltd., in Huizhou, China. Based on the collected real-world data, we evaluate the performance of EMFD. The results demonstrate that EMFD can achieve the fault diagnosis accuracy of 96% and outperforms the existing single-parameter methods.

ACKNOWLEDGMENT

This study is supported by the special fund of Guangdong frontier and key technology innovation (No. 2016B010108005), special fund of Guangdong applied science and technology research and development (No. 2016B010125001), Guangdong science and technology plan (No. 2016B090918110, 2015B010135006), National Natural Science Foundation of China under grant (No. 61672320).

REFERENCES

- [1] Y. Zheng, Y. He, M. Jin, X. Zheng, and Y. Liu, "Red: Rfid-based eccentricity detection for high-speed rotating machinery," in *Proceedings of IEEE INFOCOM*, 2018.
- [2] P. J. Rodriguez, A. Belahcen, and A. Arkkio, "Signatures of electrical faults in the force distribution and vibration pattern of induction motors," *IEEE Proceedings-Electric Power Applications*, vol. 153, no. 4, pp. 523–529, 2006.
- [3] J. Cameron, W. Thomson, and A. Dow, "Vibration and current monitoring for detecting airgap eccentricity in large induction motors," in *IEEE Proceedings B (Electric Power Applications)*, vol. 133, no. 3. IET, 1986, pp. 155–163.
- [4] F. Filippetti, G. Franceschini, C. Tassoni, and P. Vas, "Ai techniques in induction machines diagnosis including the speed ripple effect," *IEEE Transactions on Industry Applications*, vol. 34, no. 1, pp. 98–108, 1998.
- [5] A. Hajnayeb, A. Ghasemloonia, S. Khadem, and M. Moradi, "Application and comparison of an ann-based feature selection method and the genetic algorithm in gearbox fault diagnosis," *Expert Systems with Applications*, vol. 38, no. 8, pp. 10205–10209, 2011.
- [6] Y. He, J. Guo, and X. Zheng, "From surveillance to digital twin: Challenges and recent advances of signal processing for industrial internet of things," *IEEE Signal Processing Magazine*, vol. 35, no. 5, pp. 120–129, 2018.
- [7] X. Wang, D. Tan, and S. Zheng, "Application of wavelet transform for diagnosing the motor vibration signal faults of shearer haulage unit," *Coal Science and Technology Magazine*, vol. 2, no. 2, pp. 7–9, 2001.
- [8] W. Shao, J. Song, h. Ma, and m. Cao, "Design for motor diagnosis based on zigbee," *Electronic Measurement Technology*, vol. 36, no. 11, pp. 102–105, 2013.
- [9] B. Yang, "Embedded motor fault diagnosis system based on arm," Ph.D. dissertation, Donghua University, 2010.
- [10] H. Cao, X. Xu, Q. Zhu, and I. Wang, "The design and implementation of experiment platform for motor fault diagnosis based on data comprehensive acquisition system," *Large Motor Technology*, vol. 05, pp. 38–40 and 54 and 60, 2013.
- [11] M. Benbouzid, "Bibliography on induction motors faults detection and diagnosis," *IEEE Transactions on Energy Conversion*, vol. 14, no. 4, pp. 1065–1074, 1999.
- [12] E. Cabal-Yepez, A. G. Garcia-Ramirez, R. J. Romero-Troncoso, A. Garcia-Perez, and R. A. Osornio-Rios, "Reconfigurable monitoring system for time-frequency analysis on industrial equipment through stft and dwt," *IEEE Transactions on Industrial Informatics*, vol. 9, no. 2, pp. 760–771, 2013.
- [13] J. Huang, X. Hu, and Y. Gong, "A mechanical fault diagnosis method for high voltage circuit breakers based on empirical mode decomposition," *Proceedings of the Chinese Society for Electrical Engineering*, vol. 31, no. 12, pp. 108–113, 2011.
- [14] Y. Lei, J. Lin, Z. He, and M. J. Zuo, "A review on empirical mode decomposition in fault diagnosis of rotating machinery," *Mechanical Systems and Signal Processing*, vol. 35, no. 1–2, pp. 108–126, 2013.
- [15] J. Zarei and J. Poshtan, "Bearing fault detection using wavelet packet transform of induction motor stator current," *Tribology International*, vol. 40, no. 5, pp. 763–769, 2007.
- [16] J. Antonino-Daviu, S. Aviyente, E. G. Strangas, and M. Riera-Guasp, "Scale invariant feature extraction algorithm for the automatic diagnosis of rotor asymmetries in induction motors," *IEEE Transactions on Industrial Informatics*, vol. 9, no. 1, pp. 100–108, 2013.
- [17] W. Li and C. K. Mechevske, "Detection of induction motor faults: a comparison of stator current, vibration and acoustic methods," *Journal of vibration and Control*, vol. 12, no. 2, pp. 165–188, 2006.
- [18] J.-H. Jung, J.-J. Lee, and B.-H. Kwon, "Online diagnosis of induction motors using mcsa," *IEEE Transactions on Industrial Electronics*, vol. 53, no. 6, pp. 1842–1852, 2006.
- [19] W. T. Thomson, "On-line mcsa to diagnose shorted turns in low voltage stator windings of 3-phase induction motors prior to failure," in *Electric Machines and Drives Conference, 2001. IEMDC 2001. IEEE International*. IEEE, 2001, pp. 891–898.
- [20] Y. Zhao, "On-line monitoring and fault diagnosis of asynchronous motor based on stm32 devices," in *Anhui University of Science and Technology*, 2017.
- [21] W. Saadaoui and K. Jelassi, "Gearbox-induction machine bearing fault diagnosis using spectral analysis," in — *Second UKSIM European Symposium on Computer Modeling and Simulation*. IEEE, 2008, pp. 347–352.
- [22] M. M. Stopa, B. J. Cardoso Filho, and B. L. Lage, "An evaluation of the mcsa method when applied to detect faults in motor driven loads," in *IECON 2010-36th Annual Conference on IEEE Industrial Electronics Society*. IEEE, 2010, pp. 760–765.